Cádiz et al. *Advances in Continuous and Discrete Models* (2023) 2023:30
https://doi.org/10.1186/s13662-023-03774-4

Advances in Continuous and Discrete Models

RESEARCH **Open Access**

Axisymmetric self-similar finite-time singularity solution of the Euler equations

Rodrigo Cádiz[1], Diego Martínez-Argüello[1] and Sergio Rica[1*]

*Correspondence: sergio.rica@uc.cl
[1]Instituto de Física, Pontificia Universidad Católica de Chile, Avenida Vicuña Mackenna 4860, Santiago, Chile

Abstract

Self-similar finite-time singularity solutions of the axisymmetric Euler equations in an infinite system with a swirl are provided. Using the Elgindi approximation of the Biot–Savart kernel for the velocity in terms of vorticity, we show that an axisymmetric incompressible and inviscid flow presents a self-similar finite-time singularity of second specie, with a critical exponent ν. Contrary to the recent findings by Hou and collaborators, the current singularity solution occurs at the origin of the coordinate system, not at the system's boundaries or on an annular rim at a finite distance. Finally, assisted by a numerical calculation, we sketch an approximate solution and find the respective values of ν. These solutions may be a starting point for rigorous mathematical proofs.

Keywords: Euler equations; Finite-time singularity; Self-similarity

1 Introduction

The mechanics of fluids was founded by Euler more than 250 years ago. Euler described the evolution in time of an incompressible three-dimensional velocity field in three space dimensions. The fluid velocity changes according to Newton's second law, by the action of fluid pressure. Euler equations are unique because fluids obey the basic physical principles of classical mechanics, such as Galilean invariance, Newton's law, energy conservation, time-reversal symmetry, etc.

Although easy to write, these equations are hard to solve because they are partial differential equations that involve both nonlinearities and nonlocalities: The velocity changes because of pressure which itself depends on the velocity gradients in the whole space.

As a result, the general comprehension of the true nature of solutions to the Euler equations remains an open question. In particular, we have the so-called regularity problem or that of the possible existence of finite-time singularity solutions: Does a finite energy and smooth initial condition for the velocity field remain regular for all times as the velocity flow evolves in accordance with Euler equations for an inviscid and incompressible fluid? By smooth, we mean that the initial condition is differentiable everywhere. Since the early twentieth century, both mathematicians and physicists intend to answer this cumbersome problem [1].

The recent numerical observation of a potential singularity in a three-dimensional axisymetrical flow by Luo and Hou [2] on the boundary of the domain boosted intensive research from physical [3] and mathematical points of view [4]. More recently, Chen and Hou [5] have succeeded to prove the previously observed numerical singularity on the boundary domain [2].

As suggested by Pomeau and collaborators over the years [6–10], the potential connection of the putative finite-time singular solutions of Euler equations with the understanding of the intermittent behavior of turbulent motion makes the question on the existence of singular solutions of Euler equations of fundamental importance. In particular, in the framework of the focusing nonlinear Schödinger equation with small dissipation, it has been observed a scenario of potential singularities being the cause of intermittent behavior and of the anomaly of dissipation in one and two space dimensions [11, 12]. In the case of Luo and Hou, the singularity is raised on the boundaries, thus it may be a key element on the boundary layer dynamics. In a different context, by assuming a space anisotropy, one of the authors has shown that advection may cause a shock-like singularity on a circular rim of finite radius [13].

The main difficulty of Euler equations arises from the nonlocal character, however, recently, Tarek Elgindi [14] proposes a new endeavor: for a bounded vorticity distribution, the velocity field scales proportionally to spatial coordinates and the general nonlocality is reduced only to the coefficient in front. Within this approximation, Elgindi was able to find a self-similar finite-time singularity as a consequence of a nonsmooth initial condition without swirl. Contrary to Refs. [2, 5, 13], Elgindi's solution arises at a single point in the 3D space [14].

In this paper, we study a point-like finite-time singularity in the frame of the Euler equations in the axisymmetric configuration. Following Elgindi, we approximate the nonlocal dependence of the Biot–Savart law, but keep both the transport and the swirl velocity in the original Euler equations for an axisymmetric flow. Next, by expanding both the vorticity and the swirl velocity in an asymptotic series of the polar angular variable, we derive an infinite hierarchy of partial differential equations for the amplitude coefficients. Assuming a particular self-similar *Ansatz*, then the hierarchy is reduced to an autonomous set of infinitely many ordinary differential equations, in which a parameter, named ν, remains unknown. This is a "nonlinear eigenvalue" problem [15] which may be tackled via a dynamical system approach. The solution of the infinite hierarchy, together with the right boundary conditions, selects the value of ν. Finally, some special solutions are provided numerically. The numerical existence of such a solution indicates strongly the possibility of a positive existence of point-like finite-time singularities in Euler equations in an infinite domain.

The manuscript is structured as follows: in Sect. 2, by using the Elgindi approximation, the Euler equations for the axisymmetric configuration are simplified to basic model equations (7)–(10). Next, this basic model is written in spherical coordinates and projected into an infinite set of partial differential equations for the vorticity and swirl velocity amplitudes. In Sect. 3, the search for self-similar solutions transforms the original set of partial differential equations into a set of an autonomous hierarchy of ordinary differential equations, and a qualitative description of the resulting dynamical system is done. Finally, in Sect. 4, assisted by a numerical scheme of the search of solutions, the selection of the nonlinear eigenvalue ν is illustrated. To do that, the infinite hierarchy is truncated up to some order N, and a finite set of $3N$ differential equations is solved by a shooting-like method. An example of a solution is sketched for $N = 2$. Finally, we conclude.

2 Basic model

2.1 Euler equations for the axisymmetric flow

In an axisymmetric geometry, the fluid equations are simpler than in the general case. The flow is described by the three components of velocity, but no dependence is considered in the azimuthal variable ϕ. We can assume indistinctly either cylindrical or spherical coordinates. Initially, we use the cylindrical coordinates, thus $\boldsymbol{v} = (v_r(r,z,t), v_\phi(r,z,t), v_z(r,z,t))$.

The axial vorticity, ω_ϕ, and the axial velocity, v_ϕ, obey the equations [16]:

$$\left(\frac{\partial}{\partial t} + v_r\frac{\partial}{\partial r} + v_z\frac{\partial}{\partial z}\right)\omega_\phi = \frac{v_r\omega_\phi}{r} + \frac{1}{r}\frac{\partial v_\phi^2}{\partial z}, \tag{1}$$

$$\left(\frac{\partial}{\partial t} + v_r\frac{\partial}{\partial r} + v_z\frac{\partial}{\partial z}\right)v_\phi = -\frac{v_r v_\phi}{r}. \tag{2}$$

These coupled partial differential equations become self-contained if a stream function is introduced:

$$v_r = -\frac{1}{r}\frac{\partial\psi}{\partial z}, \qquad v_z = \frac{1}{r}\frac{\partial\psi}{\partial r}, \tag{3}$$

such that the velocity flow remains incompressible, and the axial vorticity component depends on terms of the stream function:

$$\omega_\phi = \frac{\partial v_r}{\partial z} - \frac{\partial v_z}{\partial r} = -\frac{1}{r}\left(\frac{\partial^2\psi}{\partial r^2} - \frac{1}{r}\frac{\partial\psi}{\partial r} + \frac{\partial^2\psi}{\partial z^2}\right). \tag{4}$$

This Poisson-like equation introduces a nonlocal dependence of the velocities, v_r and v_z, on ω_ϕ.

In conclusion, equations (1) and (2), together with (3) and (4), are formally a set of two time-dependent partial differential equations for the fields $\psi(r,z,t)$ and $v_\phi(r,z,t)$. The previous system was already numerically studied in the early 1990s [17, 18] and, more recently, but in a finite domain in [2–4].

The boundary conditions for the vorticity and the velocity are such that [2]

$$\omega_\phi(r = 0, z, t) = v_\phi(r = 0, z, t) = 0, \tag{5}$$

and, because of the condition of finite energy flow, both fields, $\omega_\phi(r = 0, z, t)$ and $v_\phi(r = 0, z, t)$, decrease to zero as $z \to \pm\infty$. Equation (2) conserves rv_ϕ thus, remarkably, if $v_\phi \geq 0$ initially, then $v_\phi \geq 0$ for all times.

2.2 Axisymmetric flow with the Elgindi approximation

By analogy with the magneto-statics, the solution of (4) is

$$\psi(r,z,t) = \frac{r}{4\pi}\int\frac{\cos\phi'}{(r'^2 + r^2 - 2r'r\cos\phi' + (z - z')^2)^{1/2}}\omega_\phi(r',z',t')r'\,dr'\,d\phi'\,dz'. \tag{6}$$

Essentially, the Elgindi approximation of the Biot–Savart law considers a punctured domain excluding the inner core, $r'^2 + z'^2 < \eta(r^2 + z^2)$, contribution to the integral which is finite because $|\omega_\phi(r', z', t)|$ remains bounded. Then the inner behavior of the integrals for the velocities is regular.[1] Finally, the contribution to the Biot–Savart integral (6) inside the punctured domain may be approximated via a multipolar expansion for $r' \gg r$ [14]. The inclusion of $\eta > 1$ ensures that it is always possible to use this multipolar approximation. Nevertheless, it results that the final singularity solution does not depend on this parameter η.

From now on, as Elgindi, we assume up–down-symmetric vorticity, $\omega_\phi(r, -z, t) = -\omega_\phi(r, z, t)$, which implies that the vertical velocity is also an odd function, $v_z(r, -z, t) = -v_z(r, z, t)$, while the radial velocity $v_r(r, -z, t) = v_r(r, z, t)$ is an even function of z. Lastly, as ω_ϕ, the swirl velocity is an odd function, $v_\phi(r, -z, t) = -v_\phi(r, z, t)$.

Following the Elgindi approximation, the radial, v_r, and vertical, v_z, velocity fields (3) become

$$v_r(r,z) \approx -r\mathcal{L}[\omega_\phi](r,z,t) \quad \text{and} \quad v_z(r,z) \approx 2z\mathcal{L}[\omega_\phi](r,z,t),$$

where the nonlocal kernel reads [14]

$$\mathcal{L}[\omega_\phi](r,z,t) = \frac{3}{4}\int_{r'^2+z'^2>\eta(r^2+z^2)} \frac{r'^2 z' \omega_\phi(r',z',t)}{(r'^2+z'^2)^{5/2}}\, dr'\, dz'. \tag{7}$$

Therefore, the final axisymmetric Euler equations simplify to

$$\frac{\partial \omega_\phi}{\partial t} + \mathcal{L}[\omega_\phi]\mathcal{D}\omega_\phi = -\omega_\phi \mathcal{L}[\omega_\phi] + \frac{1}{r}\frac{\partial v_\phi^2}{\partial z}, \tag{8}$$

$$\frac{\partial v_\phi}{\partial t} + \mathcal{L}[\omega_\phi]\mathcal{D}v_\phi = v_\phi \mathcal{L}[\omega_\phi], \tag{9}$$

where $\mathcal{D}$ is a free-scale advection or transport defined by

$$\mathcal{D} \equiv \left(-r\frac{\partial}{\partial r} + 2z\frac{\partial}{\partial z}\right). \tag{10}$$

Because (8) depends explicitly on terms of $v_\phi^2(r,z,t)$, and (9) preserves the sign of the initial condition, namely, if initially for $z > 0$, $v_\phi(r, z, t = 0)$ is nonnegative, then, $v_\phi(r, z, t)$ will be nonnegative for all times. Therefore, one defines the nonnegative function $W(r, z, t)$ by

$$v_\phi^2(r,z,t) = \left(r^2 + z^2\right)W(r,z,t). \tag{11}$$

Moreover, as already noticed by Elgindi, the Biot–Savart approximation (7) becomes simple in spherical coordinates, that is, by taking $z = \rho\cos\theta$ and $r = \rho\sin\theta$. Replacing (11) into (8) and (9), and after doing the change of variables to spherical coordinates, the equations for an axisymmetric flow become

$$\frac{\partial \omega_\phi}{\partial t} - \mathcal{L}[\omega_\phi]\mathcal{D}\omega_\phi = -\mathcal{L}[\omega_\phi]\omega_\phi - \frac{\partial W}{\partial \theta} + \frac{\cos\theta}{\sin\theta}\left(2W + \rho\frac{\partial W}{\partial \rho}\right), \tag{12}$$

[1] This property is known as electrostatic: the electric field generated by a uniform density charge is linear in coordinates, and it is neglected because it corresponds to the most regular contribution of the original singular integral.

$$\frac{\partial W}{\partial t} - \mathcal{L}[\omega_\phi]\mathcal{D}W = 2\big(2\sin^2\theta - \cos^2\theta\big)\mathcal{L}[\omega_\phi]W, \tag{13}$$

where $\mathcal{D}$ corresponds to a free scale advection linear operator defined in (10), which in spherical coordinates becomes

$$\mathcal{D} \equiv \left(3\sin\theta\cos\theta\frac{\partial}{\partial\theta} + \big(1 - 3\cos^2\theta\big)\rho\frac{\partial}{\partial\rho}\right).$$

To these equations, one needs to add the nonlocal term in spherical coordinates,

$$\mathcal{L}[\omega_\phi] = \frac{3}{4}\int_{\eta\rho}^{\infty}\frac{d\rho'}{\rho'}\int_0^{\pi}\sin^2\theta'\cos\theta'\omega_\phi\big(\rho',\theta',t\big)\,d\theta'. \tag{14}$$

Equations (12) and (13), with the nonlocal term (14), provide the basic framework for our study of the Euler equations in the axisymmetric configuration.

An important consequence of these equations is that they do not have an a priori intrinsic length scale. This has an important consequence, instead of ρ, the relevant variable will be $\log\rho$, therefore any dilation would be a translation in this log variable. Nonetheless important, neither the constant $\eta > 1$ in (14) is relevant because it is just a translation in log variables.

2.3 Series expansion in the polar angular variable in spherical coordinates

Because $\mathcal{L}[\omega_\phi]$ in (14) has no dependence on the angular variable, equations (8) and (9) are "linear" in this variable, therefore the fields ω_ϕ and v_ϕ are expanded in a series of the form

$$\omega_\phi(\rho,\theta,t) = \sum_{m=1}^{\infty}\Omega_m(\rho,t)\varphi_m(\theta) \quad \text{and} \quad W(\rho,\theta,t) = \sum_{m=1}^{\infty}W_m(\rho,t)\varphi_m(\theta), \tag{15}$$

where the amplitudes $\Omega_n(\rho,t)$ and $W_n(\rho,t)$ are functions of ρ and t, which follow a coupled set of PDEs. The special choice of the orthonormal basis $\varphi_m(\theta)$ depends on the boundary condition at the axis $r = 0$. Indeed, the axisymmetric flow requires that both original variables, $\omega_\phi(r,z,t)$ and $W(r,z,t)$, vanish on the axis of rotation $r = 0$, that is, at $\theta = 0$ and $\theta = \pi$. Moreover, because of the up–down asymmetry of the flow, only the odd modes for $\theta = \pi/2$ are considered.

We define the inner product:[2]

$$\langle f,g\rangle = \int_0^{\pi/2} f(\theta)g(\theta)\,d\theta, \tag{16}$$

such that the basis $\{\varphi_n\}$ is orthonormal, $\langle\varphi_n,\varphi_m\rangle = \delta_{nm}$.

Introducing ω_ϕ into the integral (7), we obtain

$$\mathcal{L}(\rho,t) = \sum_{m=1}^{\infty}\kappa_m\Lambda_m(\rho,t) \quad \text{with} \tag{17}$$

[2]The specific choice of basis will be discussed later on for a specific application.

$$\kappa_n = \frac{3}{2}\int_0^{\pi/2} \sin^2\theta' \cos\theta' \varphi_n(\theta')\, d\theta', \quad \text{and} \tag{18}$$

$$\Lambda_n(\rho,t) = \int_{\eta\rho}^{\infty} \frac{\Omega_n(\rho',t)}{\rho'}\, d\rho' \quad \Leftrightarrow \quad \Omega_n = -\rho\frac{\partial \Lambda_n}{\partial\rho} \quad \text{and} \quad \lim_{\rho\to\infty} \Lambda_n(\rho,t) \to 0. \tag{19}$$

The equations for the amplitudes, $\Omega_n(\rho,t)$ and $W_n(\rho,t)$, are obtained projecting equations (12) and (13) in spherical coordinates into the basis $\varphi_n(\theta)$. By multiplying (12) and (13) by $\varphi_n(\theta)$ and integrating over $\theta \in [0,\pi/2]$, one obtains an infinite matrix representation

$$\begin{aligned} &\frac{\partial}{\partial t}\Omega_n(\rho,t) + \mathcal{L}(\rho,t)\mathcal{D}_{nm}\Omega_m \\ &\quad = -\mathcal{L}(\rho,t)\Omega_n - \left(c_{nm}W_m + d_{nm}\left(2W_m + \rho\frac{\partial W_m}{\partial\rho}\right)\right), \end{aligned} \tag{20}$$

$$\frac{\partial}{\partial t}W_n(\rho,t) + \mathcal{L}(\rho,t)\mathcal{D}_{nm}W_m = \mathcal{L}(\rho,t)e_{nm}W_m, \tag{21}$$

$$\rho\frac{\partial \Lambda_n}{\partial\rho} = -\Omega_n(\rho,t), \tag{22}$$

where $\mathcal{L}(\rho,t)$ is defined in (17); moreover, we define the matrix and differential operator $\mathcal{D}_{nm}$ by

$$\mathcal{D}_{nm} = \left(a_{nm} + b_{nm}\rho\frac{\partial}{\partial\rho}\right).$$

There, the repeated indices, m, stand for the Einstein summation convention. The vector κ_n is given by (18) and the matrix elements a_{nm}, b_{nm}, c_{nm}, d_{nm}, and e_{nm} are given by

$$\begin{aligned} a_{nm} &= -3\left\langle\varphi_n, \sin\theta\cos\theta\frac{\partial\varphi_m}{\partial\theta}\right\rangle, \qquad b_{nm} = -\langle\varphi_n, (1-3\cos^2\theta)\varphi_m\rangle, \\ c_{nm} &= \left\langle\varphi_n, \frac{\partial\varphi_m}{\partial\theta}\right\rangle, \qquad d_{nm} = -\left\langle\varphi_n, \frac{\cos\theta}{\sin\theta}\varphi_m\right\rangle, \\ e_{nm} &= 2\langle\varphi_n, (2\sin^2\theta - \cos^2\theta)\varphi_m\rangle = 2(\delta_{nm} - b_{nm}). \end{aligned} \tag{23}$$

All these matrices may be computed easily for a given orthonormal basis, their elements are just numbers. Among them, b_{nm}, d_{nm}, and e_{nm} are symmetric, and c_{nm} is fully antisymmetric. Finally, a_{nm} is neither symmetric nor antisymmetric. On the other hand, a_{nm}, b_{nm}, and e_{nm} are tridiagonal, but c_{nm} and d_{nm} are fully completed by numbers. The explicit coefficients are given in the Appendix for the Fourier basis (see Eq. (41)).

3 Finite-time self-similar solution

3.1 Self-similar *Ansatz*

In the following, we look for a particular class of possible solutions of (20) and (21). Set the self-similar dependence:

$$\Omega_n(\rho,t) = \frac{1}{t_c - t}F_n\left(\frac{\rho}{(t_c-t)^\nu}\right), \tag{24}$$

$$W_n(\rho,t) = \frac{1}{(t_c-t)^2}G_n\left(\frac{\rho}{(t_c-t)^\nu}\right), \tag{25}$$

$$\Lambda_n(\rho,t) = \frac{1}{t_c - t} H_n\left(\frac{\rho}{(t_c - t)^\nu}\right), \tag{26}$$

where the self-similar rescaled variable reads

$$\xi = \frac{\rho}{(t_c - t)^\nu},$$

where $\nu > 0$ is a critical exponent to be found [15]. Furthermore, the Elgindi kernel (17) scales as

$$\mathcal{L}(\rho,t) = \frac{1}{t_c - t} L(\xi) \quad \text{with} \quad L(\xi) = \sum_{p=1}^{\infty} \kappa_p H_p(\xi). \tag{27}$$

Here the exponent ν is unknown. As it will be clarified later on, the parameter ν is a kind of a "nonlinear eigenvalue", in the sense that the solutions for $F_n(\xi)$, $G_n(\xi)$, and $H_n(\xi)$ are determined for a precise set of values for ν. This kind of self-similarity is called "2nd-kind self-similarity" [15].

Replacing the self-similar *Ansatz* into (20) and (21), one obtains

$$\begin{aligned}
&\left(F_n + \nu\xi F_n'\right) + L(\xi)\left((a_{nm} + \delta_{nm})F_m + \xi b_{nm} F_m'\right) \\
&\quad + \left(c_{nm} G_m + d_{nm}\left(2G_m + \xi G_m'\right)\right) = 0, &(28)\\
&\left(2G_n + \nu\xi G_n'\right) + L(\xi)\left((a_{nm} - e_{nm})G_m + \xi b_{nm} G_m'\right) = 0, &(29)\\
&\xi H_n' = -F_n, &(30)\\
&L(\xi) = \sum_{p=1}^{\infty} \kappa_p H_p(\xi). &(31)
\end{aligned}$$

This dynamical system must be complemented with the following boundary conditions. The outer field becomes asymptotically stationary for ρ finite and $t \to t_c$ [15]. More precisely, because of the structure of the self-similar solutions (24) and (25), the dynamics are such that both $\partial_t \Omega_n \to 0$ and $\partial_t W_n \to 0$, as $\xi \to \infty$. Therefore, the outer boundary conditions read:

$$\left(F_n + \nu\xi F_n'\right) \to 0 \quad \text{and} \quad \left(2G_n + \nu\xi G_n'\right) \to 0, \quad \text{as } \xi \to \infty, \tag{32}$$

whence

$$F_n(\xi) \approx \frac{F_n^{(\infty)}}{\xi^{1/\nu}} + \text{h.o.t.}, \qquad G_n(\xi) \approx \frac{G_n^{(\infty)}}{\xi^{2/\nu}} + \text{h.o.t.}, \qquad H_n(\xi) \approx \frac{\nu F_n^{(\infty)}}{\xi^{1/\nu}} + \text{h.o.t.} \tag{33}$$

In conclusion, in the limit $\xi \to \infty$ all variables vanish, $F_n(\xi), G_n(\xi), H_n(\xi) \to 0$.

On the other hand, for the inner region, a differentiability condition must be imposed at $\xi = 0$. Therefore, because $F_n'(0)$ and $G_n'(0)$ are finite, from the equations (28) and (29), it follows that $F_n(0) = G_n(0) = 0$ and $H_n(0) = H_n^0 \neq 0$.

3.2 Solution of the equations via dynamical system theory

As already noticed, equations (28)–(31) are free of any scale, therefore, using the variable $s = \log \xi$, one obtains an autonomous dynamical system for the hierarchy of differential equations:

$$\begin{aligned} &\big(\nu\delta_{nm} + L(s)b_{nm}\big)F'_m(s) + \big(\delta_{nm} + L(s)(a_{nm} + \delta_{nm})\big)F_m \\ &\quad + (c_{nm} + 2d_{nm})G_m + d_{nm}G'_m(s) = 0, \end{aligned} \tag{34}$$

$$\big(\nu\delta_{nm} + L(s)b_{nm}\big)G'_m(s) + \big(2\delta_{nm} + L(s)(a_{nm} - e_{nm})\big)G_m = 0, \tag{35}$$

$$H'_n(s) = -F_n, \tag{36}$$

$$L(s) = \sum_{p=1}^{\infty} \kappa_p H_p(s). \tag{37}$$

This dynamical system must be solved in view of satisfying the previously mentioned boundary conditions. Indeed, these boundary conditions correspond exactly to the fixed points of the dynamical system. On the other hand, as usual, a dynamical system as well possesses a number of singular points. Both the fixed points and the singular points will be discussed next.

3.3 Characterization of the fixed and singular points of the dynamical system

As usually happens in a dynamical system, a qualitative understanding comes from the knowledge of the attractors, in the current case the fixed points, and their stability. The fixed points of this dynamical system are characterized by a continuous family,

$$F^*_n = G^*_n = 0 \quad \text{and} \quad H^*_n \quad \text{arbitrary}.$$

A simple stability analysis indicates that the fixed point

$$F^*_n = G^*_n = H^*_n = 0 \tag{38}$$

is stable, whereas the fixed point

$$F^{(0)}_n = G^{(0)}_n = 0 \quad \text{and} \quad H^{(0)}_n \neq 0, \tag{39}$$

may be unstable for, at least, one direction.

It results that the linear stability of the stable fixed point (38) is consistent with the condition $\nu > 0$ and with the asymptotic behavior (33). On the other hand, the unstable manifold of the fixed point (39) is characterized by an eigenvalue $\sigma^* > 0$ and a nonzero perturbation along a G_n direction given by an eigenvector of the matrix $(a_{nm} - e_{nm} + \sigma^* b_{nm})$ with an eigenvalue, $-\phi$, satisfying the condition $\phi = \frac{(2+\nu\sigma^*)}{L^{(0)}}$.

Moreover, because of the differentiability of the self-similar functions at the origin $\rho = 0$ (or $\xi = 0$) [15], a supplementary condition on the most unstable eigenvalue, σ^* is required. Indeed, the asymptotic solution of (34)–(37) for $s \to -\infty$ is governed by the local behavior:

$$F_n = e^{\sigma^* s}\delta f_n, \qquad G_n(s) = e^{\sigma^* s}\delta g_n, \quad \text{and} \quad H_n(s) = H^{(0)}_n + e^{\sigma^* s}\delta h_n.$$

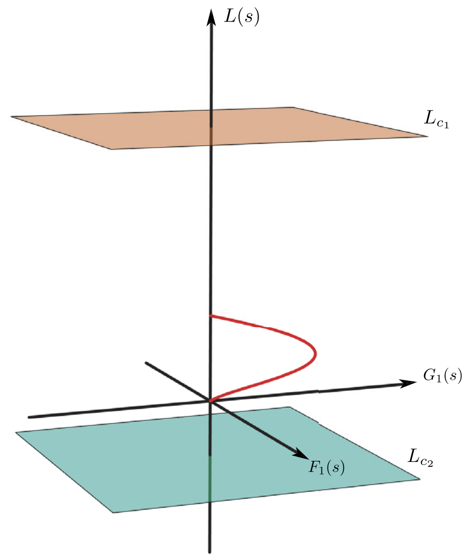

Figure 1 Plot of a 3D projection of the six-dimensional heteroclinic orbit using the axes $F_1(s)$, $G_1(s)$, and $L(s)$. This solution corresponds to the case labeled as $2^{\S}$ in the Table 1. The two planes correspond to the two singular conditions (40)

Therefore, in the original variable, near $\xi \approx 0$, all functions become power laws: $F_n = \xi^{\sigma^*}\delta f_n$, etc., thus the local behavior may not be differentiable at $\xi = 0$, unless σ^* is a positive integer,[3] that is, $\sigma^* = q$, with $q = 1, 2, 3, \dots$.

In conclusion, the pertinent solution is a heteroclinic orbit that connects, from the limit $s \to -\infty$, the unstable fixed point with the stable fixed point $F_n^* = G_n^* = H_n^* = 0$, in the limit $s \to \infty$. Up to this level, the values of the constants $H_n^{(0)}$, as well as the value of ν, must be selected by the full solution of the problem. This is illustrated in the Fig. 1 which comes from a solution for the special case to be discussed in the next section.

Besides the fixed points, the dynamical system (34) and (35) admits singular points. These are given by the points, s_*, such that

$$\det\left[\nu\delta_{nm} + L(s_*)b_{nm}\right] = 0.$$

In other words, if $\{\lambda^{(b)}\}$ denotes the set for the spectrum of the matrix b_{nm}, then the critical points are given for s_* such that $-\frac{\nu}{L(s_*)}$ belongs to the set $\{\lambda^{(b)}\}$. Because the matrix b_{nm} is symmetric, its eigenvalues are real; moreover, let $\lambda_{\max}^{(b)} > 0$ be the maximum and $\lambda_{\min}^{(b)} < 0$ the minimum eigenvalue. In general, if

$$-\frac{1}{\lambda_{\max}^{(b)}} < \frac{L(s)}{\nu} < \frac{1}{|\lambda_{\min}^{(b)}|}, \qquad \forall s \in \mathbb{R}, \tag{40}$$

then the trajectory of the solutions of the dynamical system will never cross any singular point, as sketched in Fig. 1.

[3]The condition of analyticity of all functions also implies that σ^* must be real, since a complex eigenvalue, $\sigma^* = q + i\beta$ may produce a behavior of the form $\xi^q \cos(\beta\log\xi + \delta)$ which is not regular at the origin.

3.4 Selection mechanism for the nonlinear eigenvalue ν

The linear stability of the inner solution imposes a condition for ν,

$$\phi = \frac{(2+\nu q)}{L^{(0)}},$$

where $L^{(0)} = \sum_{n=1}^{\infty} \kappa_n H_n^{(0)}$, q is an integer, and $-\phi$ is an eigenvalue of the matrix

$$(a_{nm} - e_{nm} + q b_{nm}).$$

However, the other amplitudes $\{H_n^{(0)}\}$ remain to be selected. The selection happens because of the existence of a heteroclinic orbit as a solution to the dynamical system. The search for such a heteroclinic solution of the ordinary differential equations (34)–(37) passes by a shooting-like method for the unknowns $\{H_n^{(0)}\}$, that is, by tuning the parameters $\{H_n^{(0)}\}$, to select the right solution that satisfies the right boundary conditions (32). Additionally, the function $L(s)$, defined through equation (37), has to satisfy condition (40).

Naturally, because this hierarchy is infinite, this is not an easy task. As we see in the next section, this problem may be cumbersome even for a truncation keeping a moderate number of variables. Nevertheless, some solutions do exist. In the following section, we provide a numerical example of a solution.

4 Numerical search of a solution and for the second kind similarity exponent

To solve in practice the infinite ordinary differential equations system (34)–(37), it is necessary to truncate these equations up to some order N, that is, the matrices indices run from $n = 1$ up to $n = N$. Under this assumption, a_{nm}, b_{nm}, etc., are $N \times N$ matrices, and the self-similar functions are arrays of order N. Thus, $(F_1(s), F_2(s), \ldots, F_N(s))$, $(G_1(s), G_2(s), \ldots, G_N(s))$, and $(H_1(s), H_2(s), \ldots, H_N(s))$.

For a given integer $q = 1, 2, 3 \ldots$, it is required to solve a $3N$-dimensional dynamical system that needs N independently selected parameters.

A shooting method with N parameters can be done easily for $N = 1$, and perhaps for $N = 2$, however, for higher values of N it may be a cumbersome scheme. Therefore, we use a differential evolution approach [19] to estimate the shooting parameters for the dynamical set of equations (34)–(37), together with the boundary conditions (32) as an error estimate [20].

In the following, we use a Fourier orthonormal basis with the inner product (16),

$$\varphi_n(\theta) = \frac{2}{\sqrt{\pi}} \sin(2n\theta). \tag{41}$$

In the Appendix, the specific values of the coefficients κ_n and the matrices a, b, etc., are provided. Within this basis, we have found a large number of solutions of the problem which are listed in Table 1.

Among these solutions, we notice first that for $N = 1$ the only existing solution is for $q = 1$ and $\nu = 0.89005$. Although in this case the vorticity, ω_ϕ, is differentiable, since $\omega_\phi \sim \rho \sin(2\theta)$, the swirl velocity, $v_\phi \sim \rho^{3/2} |\sin(2\theta)|$, is not differentiable more than once at the origin. Nevertheless, it is possible to relax the condition admitting to the space of solutions the initial nonnegative swirl velocities which are smooth in $v_\phi^2(r, z, t = 0)$.

Table 1 Summary of some numerically obtained solutions

N	q	# nodes	ν	$L^{(0)}$	$H_1^{(0)}$	$H_2^{(0)}$	$H_3^{(0)}$	$H_4^{(0)}$
1	$1^{\dagger}$	1	0.89005	5.7801	12.8062	–	–	–
2	$1^{\S}$	0	1.82365	1.53912	3.62004	0.73507	–	–
2	$2^{\S}$	0	1.10091	1.40061	3.13151	0.09930	–	–
2	$2^{\dagger}$	1	1.31387	1.54258	2.84748	–1.99573	–	–
3	$2^{\ddagger}$	2	1.92233	1.94822	7.17371	6.01831	23.8935	–
3	$3^{\S}$	0	0.6306	0.94388	1.85984	–0.756781	–0.31851	–
4	$2^{\ddagger}$	2	2.7186	2.47909	4.33713	–4.58815	4.88998	–4.4704
4	$2^{\ddagger}$	2	3.4453	2.9636	2.2837	–16.2556	9.9944	–6.5697

† The function $L(s)$ has a single node. Because of the oscillations, this may be called an "excited state solution" of the dynamical system.
§In this case, the function $L(s)$ has no node. Because of the simplest heteroclinic trajectory, this may be called the "ground state solution" of the dynamical system.
‡The function $L(s)$ has two nodes corresponding to a higher "excited state".

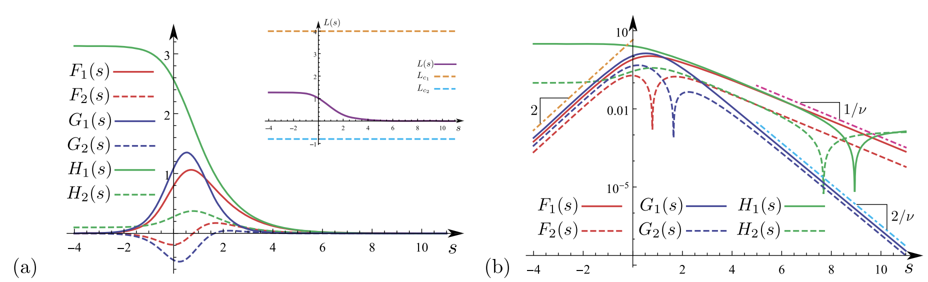

Figure 2 Numerical solutions of the system for the case $N = 2$. (**a**) Plots of the Fourier amplitudes $F_1(s)$ and $F_2(s)$ (red and red-dashed), $G_1(s)$ and $G_2(s)$ (blue and blue-dashed), and $H_1(s)$ and $H_2(s)$ (green and green-dashed). The solution selects $\nu = 1.10091$, $H_1^{(0)} = 3.13151$, and $H_2^{(0)} = 0.0993008$. (Inset) The plot of the function $L(s)$ shows that it never crosses the critical points defined by condition (40). From $L(s)$, $F_1(s)$, and $G_1(s)$, we built the 3D heteroclinic orbit of Fig. 1. (**b**) Same plot as (a) but in semilog scale, $\log|F_n(s)|$, $\log|G_n(s)|$, and $\log|H_n(s)|$ vs. s. One notices readily the exponential behavior for the inner behavior of the amplitudes $F_n(s) \sim e^{2s}$ and $G_n(s) \sim e^{2s}$. Additionally, we observe the right slopes $1/\nu$ and $2/\nu$ in the large s limit

For $N = 2$ we have observed the existence of multiple possible solutions for all $q \geq 1$. For $N = 3$ and $q = 1$, it follows that there is no suitable solution. In general, for $q = 1$ and N odd and greater than 3, we have not found any suitable solution, therefore these solutions either do not exist or are rare. A large number of solutions are obtained for $N = 4$.

Graphically we provide the particular case of $N = 2$ and $q = 2$. Figure 2(a) shows the solutions for the six amplitudes, $F_1(s)$, $F_2(s)$, $G_1(s)$, $G_2(s)$, and $H_1(s)$, $H_2(s)$, as functions of the variable, s.

Figure 2(b) shows the same plot in a semilog scale, that is, in a log–log scale if considering the original variable $\xi = \log s$. This plot clearly shows the power law behaviors as $\xi \to 0$ and $\xi \to \infty$.

As it can be seen in Fig. 2(a), the amplitudes $F_1(s)$, $G_1(s)$, and $H_1(s)$ have no nodes (zeroes), therefore, by analogy with the spectral theory of linear eigensystems, we call these solutions as the "ground states" (see the parameter solutions labeled with a § in Table 1. In the same vein, the first and second "excited states" are also obtained.

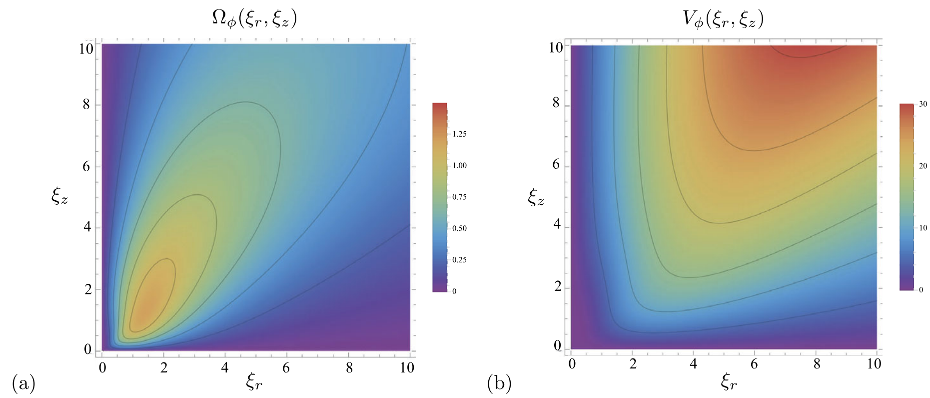

Figure 3 (**a**) The self-similar function $\Omega_\phi(\xi_r, \xi_z)$ representing the finite-time singular behavior of the vorticity field. (**b**) The self-similar function $V_\phi(\xi_r, \xi_z)$ representing the finite-time singular behavior of the swirl velocity

Finally, to represent the physical flow, Figs. 3(a) and 3(b) show the contour plots of the self-similar vorticity (a) and the self-similar swirl velocity (b), defined by

$$\Omega_\phi(\xi_r, \xi_z) = \sum_{m=1} \varphi_m(\theta) F_m(\xi) \quad \text{and} \quad V_\phi(\xi_r, \xi_z) = \xi \left(\sum_{m=1} \varphi_m(\theta) G_m(\xi) \right)^{1/2},$$

where the self-similar variables are defined in the cylindrical rescaled variables,

$$\xi_r = \xi \sin\theta \quad \text{and} \quad \xi_z = \xi \cos\theta.$$

The self-similar vorticity field, Fig. 3(a), as well as the swirl velocity, Fig. 3(b), show a global circulation in the first quadrant, in the self-similar variables (ξ_r, ξ_z). After a reconstruction of the full three-dimensional space, the main flow realized by the self-similar solution has a quadrupolar structure.

5 Conclusions and discussion

By approximating the nonlocal Biot–Savart law and projecting the axial vorticity, ω_ϕ, as well as the swirl velocity, v_ϕ, in an adequate basis, the original coupled set of partial differential equations for an axisymmetric flow is mapped into an infinite set of partial differential equations for the corresponding vorticity and swirl velocity amplitudes. The final set of nonlinear partial differential equations admits a possible finite-time self-similar behavior. The existence of this finite-time singularity is possible by the solution of an infinite system of ordinary differential equations with adequate boundary conditions.

Although the formal proof of an existing solution for the full infinite system seems to be a great challenge, the existence of such a solution may be mapped into a dynamical system problem, in which the required solution is selected by a high-dimensional shooting argument. This scheme is corroborated via the numerical solution of the original infinite dynamical system truncated up to a finite order N. We provide numerical solutions of the truncated system, indicating strong evidence of the existence of a finite-time self-similar solution of the axisymmetric Euler equations for incompressible fluids.

We end this paper with the following remarks:

1 The validity of the approximate equations (8) and (9) depends on the Elgindi approximation, that is, the contribution to the Biot–Savart integral from the inner core must be negligible regarding the full integral. In other words, the following inequality must be satisfied:

$$\left|\int_{\eta\rho}^{\infty}\frac{d\rho'}{\rho'}\int_0^{\pi/2}\sin^2\theta'\cos\theta'\omega_\phi\big(\rho',\theta',t\big)\,d\theta'\right| \gg \left|\int_0^{\eta\rho}\frac{d\rho'}{\rho'}\int_0^{\pi/2}\sin^2\theta'\cos\theta'\omega_\phi\big(\rho',\theta',t\big)\,d\theta'\right|.$$

Here the left-hand side corresponds to Elgindi approximation and the right-hand side to the inner contribution, assumed negligible. By using the series expansion (15), the inequality becomes

$$\left|\sum_{n=1}^{\infty}\kappa_n\int_{\eta\xi}^{\infty}F_n\big(\xi'\big)\frac{d\xi'}{\xi'}\right| \gg \left|\sum_{n=1}^{\infty}\kappa_n\int_0^{\eta\xi}F_n\big(\xi'\big)\frac{d\xi'}{\xi'}\right|.$$

By the results of Sect. 3.3, the value of the inner core solution of the self-similar vorticity becomes $F_n(\xi)\sim\xi^q$, therefore we conclude

$$\left|\sum_{n=1}^{\infty}\kappa_n\int_{\eta\xi}^{\infty}F_n\big(\xi'\big)\frac{d\xi'}{\xi'}\right| \gg \frac{(\eta\xi)^q}{q}\sum_{n=1}^{\infty}\kappa_n.$$

Because $\kappa_n\sim 1/n^3$, the series converges,[4] the right-hand side may be as small as desired as $\xi\to 0$, therefore, negligible regarding the Elgindi approximation.[5]

2 Neglecting advective terms, that is, whenever the matrix elements a_{nm}, b_{nm} are zero, and also setting the swirl velocity to zero ($G_n = 0$) in equations (28) and (29), makes possible finding an exact solution of the resulting self-similar equation for the vorticity (28). The resulting dynamical system simplifies to

$$F_n + \nu\xi F_n' + L(\xi)F_n = 0, \quad \text{and} \quad \xi L'(\xi) = -\sum_{p=1}^{\infty}\kappa_p F_p(s). \tag{42}$$

This infinite set of ordinary differential equations corresponds to Elgindi solution [14]. It can be integrated directly

$$L(\xi) = -\frac{2}{K\xi^{1/\nu}+1}, \tag{43}$$

which is not smooth at $\xi = 0$, unless $1/\nu$ is a positive integer, whereas Elgindi showed that advection may be discarded if and only if $1/\nu\to 0$. Nevertheless, an interesting feature of this solution is that $L(\xi = 0) < 0$, contrary to the numerically obtained solutions for the full ODE system in Sect. 4.

[4] More specifically, $\sum_{n=1}^{\infty}\kappa_n \to 0.2821\ldots$.

[5] S.R. is indebted to Isabelle Gallagher who motivated this remark.

3 Additionally, setting the swirl velocity to zero, i.e., $G_n \equiv 0\ \forall n$, the system (34)–(37) cannot be integrated analytically, but it can be solved numerically. As expected, the possible numerical solutions do not satisfy the outer boundary conditions, therefore there is no possible solution in the case of zero swirl, in agreement with Ukhovskii–Yudovich [21].

Appendix: Computation of the matrix elements

In the following, we compute explicitly the matrix elements defined in equation (23):

$$\kappa_n = 2\frac{3}{4}\int_0^{\pi/2} \varphi_n(\theta') \sin^2\theta' \cos\theta'\, d\theta' = -\frac{12n}{\sqrt{\pi}(4n^2-9)(4n^2-1)},$$

$$a_{nm} = -\left\langle \varphi_n, 3\sin\theta\cos\theta \frac{\partial \varphi_m}{\partial\theta}\right\rangle = \frac{3}{2}\begin{cases}(n+1) & \text{if } m = n+1,\\ -(n-1) & \text{if } m = n-1,\\ 0 & \text{otherwise,}\end{cases}$$

$$b_{nm} = -\langle \varphi_n, (1-3\cos^2\theta)\varphi_m\rangle = \frac{1}{4}\begin{cases}2 & \text{if } n = m,\\ 3 & \text{if } m = n+1,\\ 3 & \text{if } m = n-1,\\ 0 & \text{otherwise,}\end{cases}$$

$$c_{nm} = \left\langle \varphi_n, \frac{\partial\varphi_m}{\partial\theta}\right\rangle = \frac{4}{\pi}\frac{mn((-1)^{m+n}-1)}{(m^2-n^2)},$$

$$d_{nm} = -\left\langle \varphi_n, \frac{\cos\theta}{\sin\theta}\varphi_m\right\rangle,$$

$$e_{nm} = \langle \varphi_n, 2(2\sin^2\theta - \cos^2\theta)\varphi_m\rangle = \frac{1}{2}\begin{cases}2 & \text{if } n = m,\\ -3 & \text{if } m = n+1,\\ -3 & \text{if } m = n-1,\\ 0 & \text{otherwise.}\end{cases}$$

No simple closed expression was found for the matrix elements d_{nm}.

Acknowledgements
S.R. is indebted to Isabelle Gallagher, Michal Kowalczy, and Yves Pomeau for an interesting exchange of ideas.

Funding
This work was supported by FONDECYT (Chile) under Grant No. 1220369.

Availability of data and materials
None.

Declarations

Competing interests
The authors declare no competing interests.

Author contributions
All authors developed the mathematical framework. DMA carried out the numerical search of pertinent solutions discussed in Sect. 4. All authors analyzed the results and developed discussion. All authors read and approved the final manuscript.

Received: 16 April 2023 Accepted: 6 May 2023 Published online: 22 May 2023

References

1. Gibbon, J.D.: The three-dimensional Euler equations: where do we stand? Physica D **237**, 1894–1904 (2008)
2. Luo, G., Hou, T.Y.: Potentially singular solutions of the 3D axisymmetric Euler equations. Proc. Natl. Acad. Sci. USA **111**(36), 12968–12973 (2014). https://doi.org/10.1073/pnas.1405238111
3. Barkley, D.: A fluid mechanic's analysis of the teacup singularity. Proc. R. Soc. A, Math. Phys. Eng. Sci. **476**(2240), 20200348 (2020). https://doi.org/10.1098/rspa.2020.0348
4. Elgindi, T.M., Jeong, I.-J.: Finite-time singularity formation for strong solutions to the axi-symmetric 3D Euler equations. Ann. PDE **5**, 16 (2019)
5. Chen, J., Hou, T.Y.: Stable nearly self-similar blowup of the 2D Boussinesq and 3D Euler equations with smooth data (2022). arXiv:2210.07191
6. Pomeau, Y.: Singularité dans l'évolution du fluide parfait. C. R. Math. Acad. Sci. Paris **321**, 407–411 (1995)
7. Pomeau, Y.: On the self-similar solution to the Euler equations for an incompressible fluid in three dimensions. C. R., Méc. **346**(3), 184–197 (2018)
8. Pomeau, Y., Le Berre, M., Lehner, T.: A case of strong non linearity: intermittency in highly turbulent flows. C. R., Méc. **347**, 342–356 (2019)
9. Pomeau, Y., Le Berre, M.: Blowing-up solutions of the axisymmetric Euler equations for an incompressible fluid (2019). arXiv:1901.09426
10. Le Berre, M., Lehner, T., Pomeau, Y.: Singularities in turbulent flows: how to observe them? Phys. D, Nonlinear Phenom. **443**, 133563 (2023). https://doi.org/10.1016/j.physd.2022.133563
11. Josserand, C., Pomeau, Y., Rica, S.: Finite-time localized singularities as a mechanism for turbulent dissipation. Phys. Rev. Fluids **5**, 054607 (2020). https://doi.org/10.1103/PhysRevFluids.5.054607
12. Amauger, J., Josserand, C., Pomeau, Y., Rica, S.: Two dimensional singularity turbulence. Phys. D, Nonlinear Phenom. **443**, 133532 (2023). https://doi.org/10.1016/j.physd.2022.133532
13. Rica, S.: Potential anisotropic finite-time singularity in the three-dimensional axisymmetric Euler equations. Phys. Rev. Fluids **7**, 034401 (2022). https://doi.org/10.1103/PhysRevFluids.7.034401
14. Elgindi, T.M.: Finite-time singularity formation for $C^{1,\alpha}$ solutions to the incompressible Euler equations on $\mathbb{R}^3$. Ann. Math. **194**(3), 647–727 (2021)
15. Eggers, J., Fontelos, M.A.: Singularities: Formation, Structure, and Propagation. Cambridge Texts in Applied Mathematics. Cambridge University Press, Cambridge (2016). https://doi.org/10.1017/CBO9781316161692
16. Saffman, P.G.: Vortex Dynamics. Cambridge Monographs on Mechanics and Applied Mathematics. Cambridge University Press, Cambridge (1995)
17. Grauer, R., Sideris, T.C.: Numerical computation of 3D incompressible ideal fluids with swirl. Phys. Rev. Lett. **67**, 3511–3514 (1991). https://doi.org/10.1103/PhysRevLett.67.3511
18. Pumir, A., Siggia, E.D.: Finite-time singularities in the axisymmetric three-dimension Euler equations. Phys. Rev. Lett. **68**, 1511–1514 (1992). https://doi.org/10.1103/PhysRevLett.68.1511
19. Storn, R., Price, K.: Differential Evolution –A Simple and Efficient Heuristic for global Optimization over Continuous Spaces. Journal of Global Optimization **11**, 341–359 (1997). https://doi.org/10.1023/A:1008202821328
20. Rica, S., Ruz, G.A.: Estimating SIR model parameters from data using differential evolution: an application with Covid-19 data. In: 2020 IEEE Conference on Computational Intelligence in Bioinformatics and Computational Biology (CIBCB), pp. 1–6 (2020). https://doi.org/10.1109/CIBCB48159.2020.9277708
21. Ukhovskii, M.R., Iudovich, V.I.: Axially symmetric flows of ideal and viscous fluids filling the whole space. J. Appl. Math. Mech. **32**(1), 52–62 (1968). https://doi.org/10.1016/0021-8928(68)90147-0

Publisher's Note